et al., ibid. **116**, 10557 (1994); J. D. Petersen, S. L. Gahan, S. C. Rasmussen, S. E. Ronco, *Coord. Chem. Rev.* **132**, 15 (1994).
12. For a recent computational analysis of the electronic structure of $[Ru(bpy)_3]^{2+}$, see C. Daul, E. J. Baerends, P. Vernooijs, *Inorg. Chem.* **33**, 3538 (1994).
13. J. N. Demas and A. W. Adamson, *J. Am. Chem. Soc.* **93**, 1800 (1971) and references therein.
14. S. L. Larson, C. M. Elliott, D. F. Kelley, *J. Phys. Chem.* **99**, 6530 (1995); D. G. Johnson, *et al., J. Am. Chem. Soc.* **115**, 5692 (1993); E. Danielson, C. M. Elliot, J. W. Merkert, T. J. Meyer, *ibid.* **109**, 2519 (1987); J. C. Sauvage *et al., Chem. Rev.* **94**, 993 (1994) and references therein.
15. B. O'Regan and M. Grätzel, *Nature* **353**, 737 (1991); T. J. Meyer *et al., Inorg. Chem.* **33**, 3952 (1994).
16. This system has been examined on the picosecond time scale by several researchers. See T. Yabe *et al., J. Phys. Chem.* **94**, 7128 (1990); Y. J. Chang *et al., ibid.*, p. 729 and references therein; R. A. Malone and D. F. Kelley, *J. Chem. Phys.* **95**, 8970 (1991); L. F. Cooley, P. Bergquist, D. F. Kelley, *J. Am. Chem. Soc.* **112**, 2612 (1990). See also (*20*).
17. The laser spectrometer consists of a colliding-pulse mode-locked dye laser generating 60-fs pulses at 620 nm. The pulses are amplified to microjoule energies in a four-pass dye amplifier pumped at 540 Hz by the second harmonic of a Nd:yttrium-aluminum garnet (Nd:YAG) laser. The amplified pulses are focused through an ethylene glycol jet to generate a white light continuum. A portion of the continuum is then selected for further amplification in a second amplifier by the appropriate choice of dye. For more details, see R. W. Schoenlein, J. Y. Bigot, M. T. Portella, C. V. Shank, *Appl. Phys. Lett.* **58**, 801 (1991). For the experiments on $[Ru(bpy)_3]^{2+}$, Coumarin 480 was pumped by the third harmonic of the Nd:YAG to yield 25-fs pulses centered at 475 nm (full-width at half-maximum of 20 nm). A small portion of this pulse was redirected into an optical fiber to generate a ~10-fs probe pulse following recompression with prisms and gratings. Signals were modulated at 80 Hz, and data were collected with the use of a lock-in amplifier. Linearity of the data was confirmed using neutral density filters; the maximum observed change in transmission was typically 8%. Thirty spectra were collected at each time delay, and this cycle was repeated 20 times to afford the signal-averaged data.
18. A crystalline sample of $[Ru(bpy)_3](PF_6)_2$ was prepared by metathesis of commercially available $[Ru(bpy)_3]Cl_2$ (Aldrich) with NH_4PF_6 in aqueous solution, followed by two recrystallizations via diffusion of diethyl ether into CH_3CN that had been freshly distilled over CaH_2 and thoroughly degassed. Purity of the final product was checked by high-performance liquid chromatography, which gave a single peak, and elemental analysis indicating that the isolated compound was free of cocrystallized solvent. A static emission spectrum and nanosecond time-resolved emission data further confirmed the single-component nature of the sample. The sample was dissolved in dry, distilled CH_3CN and placed in a 0.2-mm pathlength cell (optical density = 0.6 at 475 nm). Absorption spectra of the sample measured before and after collection of a full data set were completely superimposable, indicating that there had been no significant photodegradation of the compound over the course of the experiment. Independent measurements made on different samples gave identical results. Data collected on the pure CH_3CN solvent showed signals attributable to cross-phase modulation between the pump and probe beams, but the relative amplitude of these signals were only about 10 to 15% that of $[Ru(bpy)_3]^{2+}$ and do not significantly affect the data illustrated in Fig. 2.
19. N. H. Damrauer, T. R. Boussie, M. Devenney, J. K. McCusker, unpublished results.
20. N. Sutin and C. Creutz, *Adv. Chem. Ser.* **168**, 1 (1978); N. Sutin, *Photochemistry* **80**, 97 (1979); C. Creutz, M. Chou, T. L. Netzel, M. Okumura, N. Sutin, *J. Am. Chem. Soc.* **102**, 1309 (1980).
21. It is difficult to assess vibrational relaxation dynamics given the broad, somewhat featureless nature of electronic absorption spectra. However, because charge-transfer spectra are particularly sensitive to changes in molecular structure, it is reasonable to assume that most of the structural rearrangement in the system is complete by Δt = 300 fs.
22. S. J. Rosenthal, X. Xie, M. Du, G. Fleming, *J. Chem. Phys.* **95**, 4715 (1991).
23. P. V. Kumar and M. Maroncelli, *ibid.* **103**, 3038 (1995) and references therein; M. Maroncelli, *ibid.* **94**, 2084 (1991); D. McMorrow and W. T. Lotshaw, *ibid.* **95**, 10395 (1991).
24. Y. K. Shin, B. S. Brunschwig, C. Creutz, N. Sutin, *J. Phys. Chem.* **100**, 8157 (1996) and references therein.
25. Although there is nothing known about the vibrational modes which couple to the $^1MLCT \rightarrow {}^3MLCT$ conversion, it is known that the C–C stretch of the bpy ring ($\hbar\omega \approx 1400\ cm^{-1}$) is strongly coupled to the $^3MLCT \rightarrow {}^1A_1$ relaxation process.
26. A similar proposal has been put forth to explain ultrafast $^1MLCT \rightarrow {}^5T_2$ conversion in a spin-crossover complex, although the time resolution was insufficient to observe the actual formation of the low-energy excited state. See J. K. McCusker, *et al., J. Am. Chem. Soc.* **115**, 298 (1993).
27. A. Vlcek Jr., *Chemtracts-Inorg. Chem.* **5**, 92 (1993).
28. This research was supported by the University of California (J.K.M.), the ACS-PRF grant 31016-G6 (J.K.M.), and the U.S. Department of Energy, contract DE-AC0376SF00098 (C.V.S.). G.C. acknowledges support from a NATO fellowship.

23 July 1996; accepted 29 October 1996

Effects of Monomer Structure on Their Organization and Polymerization in a Smectic Liquid Crystal

C. Allan Guymon, Erik N. Hoggan, Noel A. Clark, Thomas P. Rieker, David M. Walba, Christopher N. Bowman*

Photopolymerizable diacrylate monomers dissolved in fluid-layer smectic A and smectic C liquid crystal (LC) hosts exhibited significant spatial segregation and orientation that depend strongly on monomer structure. Small, flexible monomers such as 1,6-hexanediol diacrylate (HDDA) oriented parallel to the smectic layers and intercalated, whereas rod-shaped mesogen-like monomers such as 1,4-di-(4-(6-acryloyloxyhexyloxy)benzoyloxy)-2-methylbenzene (C6M) oriented normal to the smectic layers and collected within them. Such spatial segregation caused by the smectic layering dramatically enhanced photopolymerization rates; for HDDA, termination rates were reduced, whereas for C6M, both the termination and propagation rates were increased. These polymerization precursor structures suggest novel materials-design paradigms for gel LCs and nanophase-separated polymer systems.

In pursuit of novel LC phase behavior and properties, a number of polymer-LC composites have been developed. Some composites make use of LC polymers (*1*), whereas others are formed by phase separation of the polymer and LC to produce LC droplets [polymer-dispersed LCs (PDLCs) (*2, 3*)]. Another group of these composites that show great promise is formed by the polymerization of monomer solutes in an LC solvent (*4*). These polymer-LC gel systems can yield electro-optically bistable chiral nematic devices [polymer-stabilized LCs (PSLCs) (*5*)] and ferroelectric LC gels [(PSFLCs) (*6, 7*)], which combine fast electro-optic response (*8*) with polymer-induced mechanical stabilization (*9*). Research to date on the formation and structure of polymer-LC gels has focused on the macroscopic phase behavior and optical properties of the resulting composites (*10*). Little is known, however, about the roles that the monomer segregation and subsequent polymerization behavior play on the ultimate performance of the polymer-LC gel.

We report results on the effect of diacrylate monomer structure on the spatial organization of monomer-LC mixtures prior to polymerization and thus the effect of monomer segregation and structure on polymerization kinetics. This work was initially motivated by observations of a dramatically enhanced rate of photopolymerization of LC acrylate monomers (*11*) and decreased termination rate (*12*) in LC phases, which suggests that the inherent order in LCs can significantly alter chemical reaction behavior and kinetics (*13*). The fluidlike environment in LCs not only permits molecular motion, diffusion, and chemical reaction, but also is both spatially anisotropic (orientational ordered) and spatially inhomogeneous (for example, layered). We find distinctive structure-dependent positional and orientational ordering of the monomers in which small flexible monomers intercalate between smectic layers and mesogenic

C. A. Guymon, E. N. Hoggan, C. N. Bowman, Department of Chemical Engineering, University of Colorado, Boulder, CO 80309–0424, USA.
N. A. Clark, Department of Physics, University of Colorado, Boulder, CO 80309–0390, USA.
T. P. Rieker, Department of Chemical and Nuclear Engineering, Center for Micro-Engineered Materials, University of New Mexico, Albuquerque, NM 87106, USA.
D. M. Walba, Department of Chemistry, University of Colorado, Boulder, CO 80309–0215, USA.
*To whom correspondence should be addressed.

monomers segregate within them. We also observe structure-dependent effects on the polymerization processes.

The smectic LC was a 1:1 mixture of W7(**1**) and W82(**2**) that has isotropic (I), smectic A* (SA*), smectic C* (SC*), and crystal (X) phases [I ↔ 58°C ↔ SA* ↔ 48°C ↔ SC* ↔ 13°C ↔ X] (6). The two monomers we studied were 1,6-hexanediol diacrylate (HDDA, **3**) and 1,4-di-(4-(6-acryloyloxyhexyloxy)benzoyloxy)-2-methylbenzene (C6M, **4**) (Scheme 1) (*14*). C6M is rod-shaped and has neat I, nematic (N), and X phases [I ↔ 116°C ↔ N ↔ 86°C ↔ X], whereas HDDA is a highly flexible molecule having a single I fluid phase.

To investigate the effects of LC phase and temperature on polymerization, the normalized polymerization rate was determined as a function of double-bond conversion for initiation in various LC phases with a differential scanning calorimeter equipped with a photocalorimetric accessory. Systems containing up to 2 weight % of HDDA or 6 weight % C6M dissolved in the LC solvent were polymerized at temperatures within the I, SA*, and SC* solvent LC phases

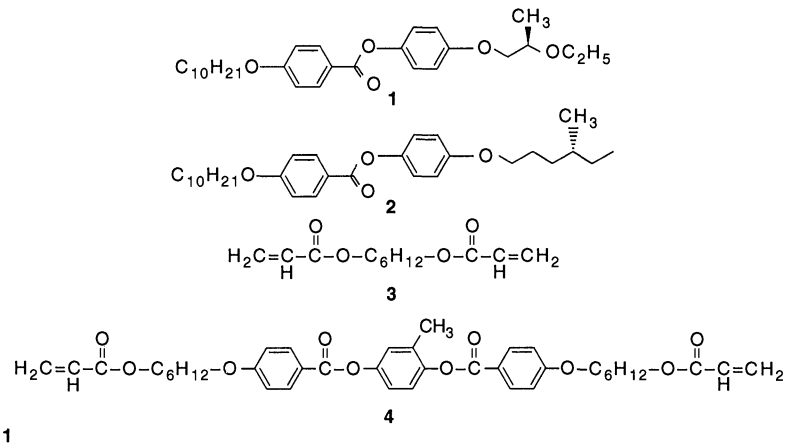

Scheme 1

(Fig. 1). The addition of these monomers changed the phase transitions of the system to a limited extent. For example, adding 2 weight % HDDA decreased the I ↔ SA* transition <1°C and the SA* ↔ SC* transition ~3°C. The polymerization temperatures, however, were chosen so that the polymerizations take place almost exclusively in the indicated phase. Interestingly, and in contrast to behavior generally found in isotropic solvents, as temperature decreased, the polymerization rate increased significantly for both HDDA and C6M. The maximum rate observed for HDDA in the SC* phase was about three times that observed in the I phase of the LC and almost six times greater than that seen in an isotropic solvent (*15*) showing reactivity quite similar to that seen in polymerization of neat LC diacrylates (*11*). Thus, for two monomers with vastly different structure and mesogenic properties, a dramatic increase in the polymerization rate was observed as the LC order of the solvent increases.

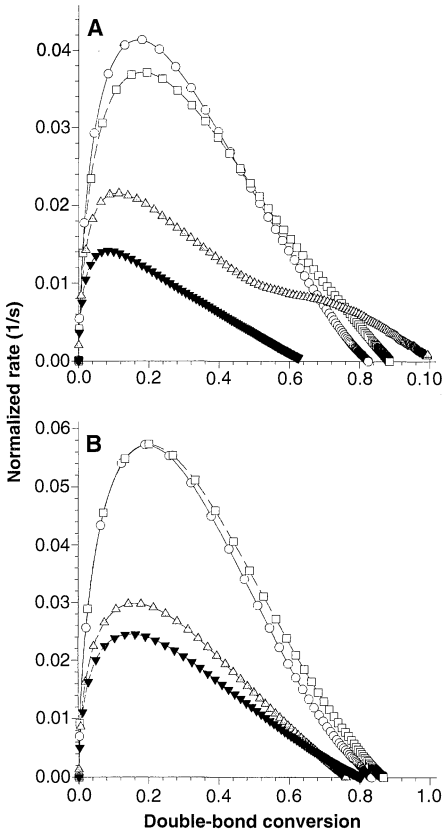

Fig. 1. Photopolymerization rate as a function of double-bond conversion for (**A**) 2% HDDA in W7,W82 in SC* at 35° (○) and 45°C (□), in SA* at 54°C (△), and in I at 70°C (▼), and (**B**) 6% C6M in SC* at 25° (○) and 40°C (□), in SA* at 56°C (△), and in I at 70°C (▼).

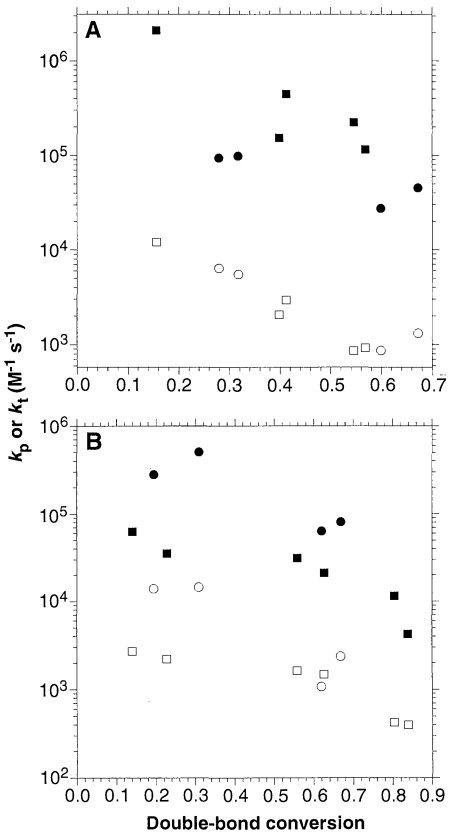

Fig. 2. (**A and B**) The photopolymerization kinetic constants k_p at 23°C, SC* (○), and 65°C, I (□), and k_t at 23°, SC* (●), and 65°C, I (■) for polymerization of (A) 5% HDDA and (B) 6.2% C6M in W7,W82.

The propagation and termination kinetic constants for polymerization, k_p and k_t, respectively, were determined from aftereffect experiments (*16*) (Fig. 2). The rate of photoinitiation was assumed to be independent of LC phase and temperature (*15*). For HDDA polymerization, k_p, shown in Fig. 2A, depended little on the phase or temperature; however, k_t was almost an order of magnitude lower in the SC* phase at lower conversions and remained depressed throughout the reaction, strongly resembling the behavior seen in polymerizations of pure LC diacrylates (*12*). In these systems, a reduced k_t leads to higher radical concentrations and thus higher polymerization rates. In contrast, for C6M (Fig. 2B), k_p and k_t are almost an order of magnitude greater in the SC* than in the I phase, leading to an overall increase in the polymerization rate (*17*). The increase in k_p and k_t likely arises from an anisotropic distribution of both radicals and double bonds. If the reactive double bonds are concentrated in a reduced volume, then the effective concentration of the double bonds (and the radicals as well) is much higher than the bulk concentration, which would result in an increase in the apparent k_p and k_t.

Infrared (IR) dichroism and x-ray diffraction (XRD) studies were used as more direct probes of the organization of the monomers in the LC environment. Molecular orientation in single-domain samples

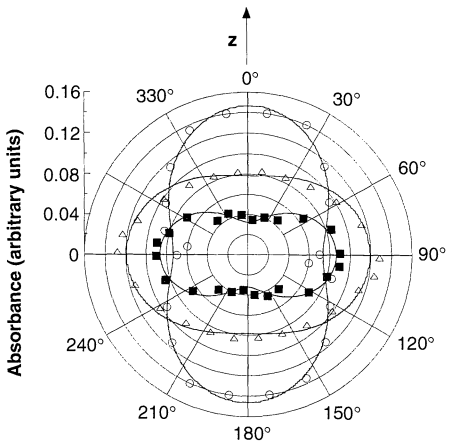

Fig. 3. Polar plot of the absorbance $A(\Psi)$ of the IR band for the acrylate C=C stretch at 1635 cm^{-1} for 5% HDDA (■) and 15% C6M (○) in W7,W82. The scaled (1:15) absorbance $A(\Psi)$ is also given for the C=O stretch in W7,W82 at 1732 cm^{-1} (△). All of the samples were introduced between two rubbed nylon-coated CaF_2 cells for examination. The monomer-LC sample cells were separated with 10-μm spacers, whereas the LC sample cells used 1-μm spacers.

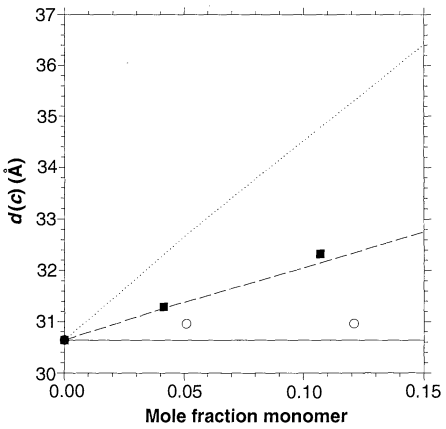

Fig. 4. Smectic layer spacing d for samples of HDDA (■) and C6M (○) in W7,W82 as a function of concentration. The dotted (C6M) and dashed (HDDA) lines correspond to d if all of the molecules intercalated between the smectic layers, whereas the solid line corresponds to d if all of the molecules segregated into the smectic layers.

can be determined by IR dichroism, which probes the orientation of bond-vibration absorption dipoles (*18*, *19*). In the HDDA or C6M/W7,W82 mixtures, only the HDDA and C6M have acrylic C=C groups and thus uniquely contribute the C=C stretching peak at 1635 cm^{-1} to the IR spectrum. Figure 3 shows polar plots of $A_{1635}(\Psi)$, the absorbance of the 1635-cm^{-1} peak, versus Ψ, or polarization angle, for 5 weight % HDDA and 15 weight % C6M in W7,W82, along with $A_{1735}(\Psi)/15$, the scaled absorbance of the W7,W82 carbonyl vibration for comparison of the C=C orientation with a moiety in the LC. The $A_{1635}(\Psi)$ data indicate that the HDDA acrylic double bonds are oriented primarily parallel to the layers, whereas the C6M moieties are oriented primarily normal to the layers. The dichroic ratios (~2:1) show that in both cases the orientational ordering is substantial.

Further insight into monomer organization can be obtained from powder XRD measurements of the dependence of smectic layer spacing, $d(c)$ (*20*), on monomer concentration (Fig. 4). For each monomer, the dashed (HDDA) and dotted (C6M) lines are $d(c)$ calculated under the assumption that all of the solute monomer molecules are intercalating between the smectic layers and contributing their volume to a layer-spacing increase. The solid line is $d(c)$ calculated under the assumption that all of the solute monomer molecules are segregating into the smectic layers, contributing to an increase in the layer area but adding nothing to the layer spacing. The results again show dramatic differences between HDDA and C6M, with HDDA apparently swelling the layers by the amount corresponding to complete interlayer intercalation and the C6M only in increasing layer area, corresponding to complete intralayer segregation.

The IR and XRD results allow us to propose models for the organization of HDDA and C6M in the W7,W82 solvent (Fig. 5). The HDDA monomers are parallel to the layers and in sheets that space the smectic layers and form an organic lyotropic structure (*20*). The C6M monomers mimic the LC molecules and mix within the smectic layers. These organizational features produce the dependence on LC order of the polymerization kinetics, which affects the ultimate polymer characteristics such as structure, solubility, and elasticity of the polymer-LC gels. The polymerization of these systems will be significantly different because of the initial monomer distribution and will result in networks with dramatically different morphologies.

This work suggests that copolymerization of monomers with distinctive segregation and orientation behavior could be used to form polymers with controlled nanostructures. For example, mixtures of mono- and diacrylate homologs of HDDA should enable the synthesis of two-dimensional elastomeric sheets, which could then be pinned together by mesogenic diacrylates to form a three-dimensional elastomeric lamellar polymer structure, akin to a cross-linked side-chain polymer-monomer LC mixture. Such a scheme offers a basic advantage over side-group polymers in that it effectively decouples the chemistry of polymerization and the properties of the polymer from those of the LC, the latter of which can be independently optimized (*21*).

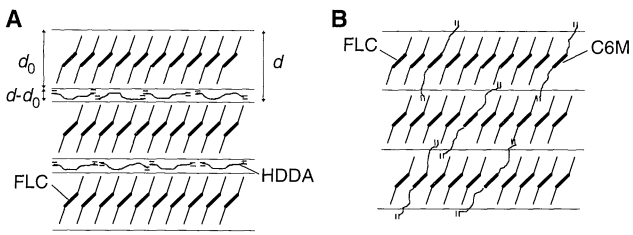

Fig. 5. Proposed models for the segregation of (**A**) HDDA and (**B**) C6M in W7,W82. The HDDA molecules segregate in between the smectic layers confining the molecules and increasing the layer spacing, whereas the C6M molecules transverse the smectic layers concentrating the double bonds.

REFERENCES AND NOTES

1. D. J. Broer and G. N. Mol, *Makromol. Chem.* **190**, 19 (1989).
2. H.-S. Kitzerow, *Liq. Cryst.* **16**, 1 (1994).
3. P. S. Drzaic, *Liquid Crystal Dispersions* (World Scientific, Singapore, 1995).
4. R. A. M. Hikmet and M. Michielsen, *Adv. Mater.* **7**, 300 (1995).
5. D. K. Yang, L. C. Chien, J. W. Doane, *Appl. Phys. Lett.* **60**, 3102 (1992).
6. C. A. Guymon, E. N. Hoggan, D. M. Walba, N. A. Clark, C. N. Bowman, *Liq. Cryst.* **19**, 719 (1995).
7. R. A. M. Hikmet, H. M. J. Boots, M. Michielsen, *ibid.*, p. 65.
8. D. M. Walba, *Science* **270**, 250 (1995).
9. G. Lester, H. Coles, A. Murayama, M. Ishikawa, *Ferroelectrics* **148**, 389 (1993).
10. R. A. M. Hikmet and H. M. J. Boots, *Phys. Rev. E* **51**, 5824 (1995).
11. C. E. Hoyle and C. P. Chawla, *Macromolecules* **28**, 1946 (1995).
12. C. E. Hoyle and T. Watanabe, *ibid.* **27**, 3790 (1994).
13. R. G. Weiss, *Tetrahedron* **44**, 3413 (1988).
14. D. J. Broer, R. A. M. Hikmet, G. Challa, *Makromol. Chem.* **190**, 3201 (1989).
15. C. A. Guymon, E. N. Hoggan, C. N. Bowman, unpublished results.
16. K. S. Anseth, L. M. Kline, T. A. Walker, K. J. Anderson, C. N. Bowman, *Macromolecules* **28**, 2491 (1995).
17. C. N. Bowman, K. S. Anseth, C. M. Wang, *Polymer* **35**, 3243 (1994).
18. C. E. Hoyle, T. Watanabe, J. B. Whitehead, *Macromolecules* **27**, 6581 (1994).
19. W. G. Jang, C. S. Park, J. E. MacLennan, K. H. Kim, N. A. Clark, *Ferroelectrics* **180**, 213 (1996).
20. T. P. Rieker, *Liq. Cryst.* **19**, 497 (1995).
21. C. A. Guymon, L. A. Dougan, E. N. Hoggan, C. N. Bowman, in preparation.

22. We thank the Department of Defense for its support of this work through a fellowship to CAG and D. Broer for generously providing the C6M monomer. The financial support of the National Science Foundation (MRG grant DMR-9224168 and CTS-9453369) and help with the IR dichroism from W. Jang is also gratefully acknowledged.

22 July 1996; accepted 31 October 1996